# Effect of flow rate and constant operating current on the behaviour of a recirculating electrochemical reactor system*

L. H. MUSTOE

*Department of Chemical Engineering, Loughborough University of Technology, Loughborough, Leicestershire, UK*

A. A. WRAGG

*Department of Chemical Engineering, University of Exeter, Exeter, Devon, UK*

A theoretical analysis is presented for the current–time, voltage–time and power–time relationships and for the energy requirement and process time for the cathodic extraction of copper in a porous flow-through electrode operated as a batch recirculation system under galvanostatic conditions. The anode reaction considered is $O_2$ evolution and the secondary cathode reaction is $H_2$ evolution. The copper extraction is under diffusion control, plug flow is assumed in the reactor and perfect mixing in the reservoir. Comparison is made with the case of operation at the limiting current throughout the process duration.

## Nomenclature

| | |
|---|---|
| $A$ | Cross-sectional area ($m^2$) |
| $a$ | specific surface area ($m^{-1}$) |
| $a_a, b_a$ | Tafel constants for anode (V) |
| $a_H, b_H$ | Tafel constants for hydrogen evolution (V) |
| $C$ | concentration ($mol\, m^{-3}$) |
| $C_0$ | concentration in reservoir or at reactor inlet ($mol\, m^{-3}$) |
| $C_0^0$ | concentration in reservoir at $t = 0$ ($mol\, m^{-3}$) |
| $C_L$ | concentration leaving reactor ($mol\, m^{-3}$) |
| $C_s$ | concentration at electrode surface ($mol\, m^{-3}$) |
| $d$ | particle diameter (m) |
| $E$ | specific energy consumption ($J\, kg^{-1}$) ($kWh\, kg^{-1}$ in Figures) |
| $F$ | Faraday's constant ($C\, mol^{-1}$) |
| $g$ | gravitational acceleration ($m\, s^{-2}$) |
| $H$ | height of reactor system for $\Delta p$ (m) |
| $I_L$ | limiting current (A) |
| $I$ | operating current (A) |
| $i$ | current density (superficial) ($A\, m^{-2}$) |
| $i_C$ | current density of primary reaction ($A\, m^{-2}$) |
| $i_H$ | current density of hydrogen evolution ($A\, m^{-2}$) |
| $k$ | mass transfer coefficient ($m\, s^{-1}$) |
| $L$ | reactor bed length (m) |

| | |
|---|---|
| $M_w$ | molecular weight (kg mol$^{-1}$) |
| $P$ | power (W) |
| $\Delta p$ | pressure drop (N m$^{-2}$) |
| $Q$ | flow rate (m$^3$ s$^{-1}$) |
| $R_f$ | final desired degree of conversion |
| $R'$ | gas constant (J K$^{-1}$ mol$^{-1}$) |
| $Re$ | Reynold's number ($udp/\mu$) |
| $Sc$ | Schmidt number ($\mu/\rho D$) |
| $S_e$ | electrode separation (m) |
| $T$ | temperature of electrolyte (K) |
| $t$ | time (s) |
| $t_1$ | time defined by Equation 11 (s) |
| $t^{90}$ | time for 90% conversion in reservoir (s) |
| $t_P$ | process time (h kg$^{-1}$ on diagrams) (s kg$^{-1}$) |
| $u$ | superficial flow velocity (m s$^{-1}$) |
| $V$ | total cell voltage (V) |
| $V_{min}$ | decomposition potential (V) |
| $V_R$ | reservoir volume (m$^3$) |
| $x$ | distance in flow direction (m) |
| $z$ | valency |

Greek characters

| | |
|---|---|
| $\alpha$ | defined by Equation 1 |
| $\beta$ | defined by Equation 2 |
| $\gamma$ | solution conductivity in bed (ohm$^{-1}$ m$^{-1}$) |
| $\gamma_0$ | bulk solution conductivity (ohm$^{-1}$ m$^{-1}$) |
| $\epsilon$ | voidage |
| $\eta_a$ | anode activation overpotential (V) |
| $\eta_{conc, L}$ | concentration overpotential at $x = L$ (V) |
| $\tau$ | reservoir residence time (s) |
| $\phi_s$ | solution potential (V) |
| $\Delta\phi_{ohm}$ | ohmic potential drop between electrodes (V) |
| $\Delta\phi_s$ | solution potential drop in cathode (V) |
| $\mu$ | viscosity (N s m$^{-2}$) |
| $\rho$ | density (kg m$^{-3}$) |
| $\xi$ | efficiency factor for pumping power |

## 1. Introduction

The behaviour of an electrochemical reactor with batch recirculation of the electrolyte has been analysed using a simple theoretical model. The system is shown in Fig. 1. The process considered is the cathodic removal of metal ions from an aqueous solution in a porous electrode under conditions of diffusion control. Such conditions are encountered in the treatment of effluents from metal treatment plants where a high concentration of swamping electrolyte is present. Plug flow conditions are assumed in the reactor and the reservoir is considered as a perfectly stirred tank.

For a batch recirculation system operated at controlled potential so that the instantaneous limiting current is maintained throughout the process, the continuous change in input concentration to the reactor results in both the applied current and the applied voltage decreasing with time.

One alternative is to operate so that the cell current is constant and below the value of the initial limiting current (Fig. 2). For part of the process duration the operating current lies below the instantaneous limiting current, and this represents an under-utilisation of reactor capacity. When the operating
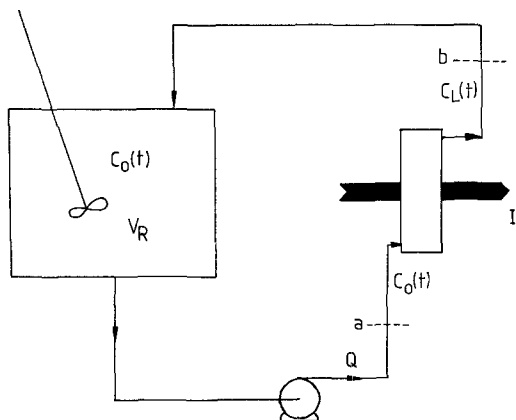
Fig. 1. Batch recirculation single reactor system with constant current. $\Delta p$ taken between 'a' and 'b'.

current exceeds the instantaneous limiting current, secondary reactions (such as $H_2$ evolution) must commence resulting in power wastage. The metal ions continue to be removed but at a gradually decreasing rate corresponding to the instantaneous limiting current. In this paper such a method of operation is considered and the effect of recirculation rate and current on the variation of reservoir concentration and cell voltage is determined. Together with energy consumption and process times these results are compared with those obtained for a system operated at the limiting current throughout. This problem was briefly discussed for a two-module reactor in an earlier paper [1].

## 2. Concentration and current–time behaviour

The initial limiting current, $I_L^0$, at time $t = 0$, provides a covenient means for specifying the constant operating current, $I$. That is:

$$I = \alpha I_L^0 \qquad 0 < \alpha < 1 \tag{1}$$

Provided $I < I_L$ a current efficiency of 100% has been assumed. It would be relatively simple to allow for a lower current efficiency provided this does not depend on the current. For a plug flow reactor the relationship between outlet and inlet concentration for operation at the limiting current is
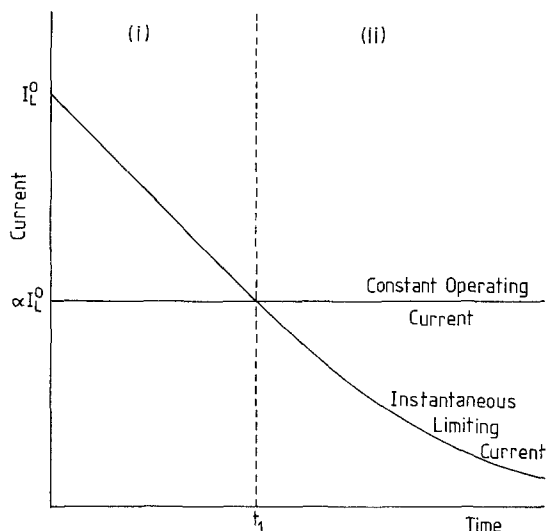
$$C_L(t) = C_0(t)\beta \tag{2}$$



Fig. 2. Schematic current–time curves showing operating regions.

where

$$\beta = \exp\{-kaL/u\}$$

The time variation of the reservoir (or cell inlet) concentration may be easily shown [2] then to be

$$C_0(t) = C_0^0 \exp\left\{-\frac{t}{\tau}(1-\beta)\right\} \tag{3}$$

The limiting current is given in general by

$$I_L(t) = zFQC_0(t)(1-\beta) \tag{4}$$

Since the limiting current as predicted by Equation 4 falls with time, operation at constant current will mean that two operating regions will exist as in Fig. 2. When $\alpha I_L^0 < I_L(t)$ there is effectively sub-limiting current operation, and some of the reactor capacity is under-used (region (i) in Fig. 2). When $\alpha I_L^0 \geqslant I_L(t)$, the primary reaction is proceeding under limiting current conditions, though as the time increases the proportion of the current being wasted on secondary reactions will also increase, (region (ii) of Fig. 2).

For the initial operating region ($\alpha I_L^0 < I_L(t)$) the reactor exit concentration is given by

$$C_L = C_0 - \frac{\alpha I_L^0}{zFQ} \tag{5}$$

which, using Equation 4 for the initial limiting current, may be written as

$$C_L = C_0 - \alpha C_0^0(1-\beta) \tag{6}$$

A mass balance on the reservoir yields

$$V_R \frac{dC_0(t)}{dt} = Q(C_L - C_0) \tag{7}$$

which upon combination with Equation 6 yields

$$\frac{dC_0(t)}{dt} = \alpha C_0^0 \frac{(1-\beta)}{\tau} \tag{8}$$

Integration from $t = 0$ time $t$ then gives

$$C_0(t) = C_0^0\left[1 - \frac{\alpha t}{\tau}(1-\beta)\right] \tag{9}$$

This equation relates the reservoir concentration at time $t$ to the initial concentration provided $\alpha I_L^0 < I_L(t)$. The time at which $\alpha I_L^0 = I_L(t)$ is also that at which

$$\alpha C_0^0 = C_0(t) \tag{10}$$

so that substituting for $C_0(t)$ from Equation 9, the upper limit of $t$ for this region of operation is

$$t_1 = \tau(1-\alpha)/\alpha(1-\beta) \tag{11}$$

When this time has been reached and exceeded, a secondary reaction occurs, the primary reaction may be considered to proceed at a rate represented by the instantaneous limiting current and Equation 2 may be used. In this case a mass balance on the reservoir leads to the equation

$$\frac{dC_0(t)}{dt} = \frac{C_0(t)}{\tau}(1-\beta) \tag{12}$$

This equation does not apply from $t = 0$ but from the time given by Equation 11 when the concentration is given by Equation 12 so that the integration to be performed is:

$$\int_{\alpha C_0^0}^{C_0(t)} \frac{dC_0(t)}{C_0(t)} = -\int_{t_1}^{t} \frac{(1-\beta)}{\tau} dt \tag{13}$$

giving:

$$C_0(t) = \alpha C_0^0 \exp\left[ -(1-\beta)\frac{t}{\tau} - \frac{1-\alpha}{\alpha} \right] \tag{14}$$

This equation predicts the concentration–time relationship in the time region

$$\frac{\tau(1-\alpha)}{\alpha(1-\beta)} < t < \infty \tag{15}$$

Thus Equations 9 and 14 predict the concentration–time behaviour of the reactor system.

## 3. Voltage requirements

### 3.1. *Basic equations*

The overall cell potential is governed by the values of solution potential drop both between the electrodes and within a porous electrode, concentration overpotential terms, surface (or activation) overpotential terms and the decomposition potential (where the anode reaction is not the reverse of the cathode reaction).

Other factors which need to be considered include whether or not the instantaneous limiting current has been exceeded and the relative positions of the anode and cathode in relation to the flow direction. Initially equations will be developed which apply to operation under limiting current conditions. The superficial current density within the cathode, $i$, can be related to the potential gradient by Ohm's law so that

$$i = -\gamma \frac{d\phi s}{dx} \tag{16}$$

For an upstream counter-electrode with the boundary condition $i = 0$ at $x = L$, the solution potential drop in the cathode, as shown by Newman and Tiedemann [3] and Pickett [4], is ;

$$\Delta\phi_s = \frac{zFu^2 C_0}{ka\gamma} \left[ \left(1 + \frac{kaL}{u}\right) \exp\left(-\frac{kaL}{u}\right) - 1 \right] \tag{17}$$

Assuming the anode reaction ($O_2$ evolution) has Tafel characteristics and that the potential drop in the solution between the electrodes obeys Ohm's law

$$\Delta\phi_{ohm} = iS_e/\gamma_0 \tag{18}$$

where $\gamma_0$, the conductivity of the bulk solution, is related to the conductivity within the electrode, $\gamma$, by

$$\gamma = \gamma_0 \epsilon^{1.5} \tag{19}$$

then the resultant overall potential drop for an upstream counter-electrode [5] is:

$$V = V_{min} + a_a + b_a \ln i + (iS_e/\gamma_0) + |\Delta\phi_s| + |\eta_{conc,L}| \tag{20}$$

where the last two terms represent a cathodic contribution to the overall potential drop. The concentration overpotential may be found from

$$\eta_{conc,L} = \frac{R'T}{zF} \ln \frac{Cs}{C} \tag{21}$$

and in calculations at or above the instantaneous limiting current the ratio $C_s/C$ is arbitrarily set to 0.001 as an approximation to limiting current conditions when $C_s \to 0$.

### 3.2. *Operation above instantaneous limiting current*

The voltage given by Equation 20 is that required to force the copper deposition reaction onto its diffusion plateau. When the operating current exceeds the instantaneous limiting current corresponding to this plateau the cell voltage increases by an additional activation overpotential term for the secondary reaction, considered here to be hydrogen evolution. The current may then be considered as having two components:

$$i = i_C + i_H. \tag{22}$$

With time $i_C$, the instantaneous limiting current, falls and $i_H$ rises so that the overall value, $i$, is constant. The fall in $i_C$ corresponds to a fall in reservoir concentration and hence in the solution potential drop due to the primary reaction. The value of $V$ given by Equation 20 under these conditions will thus fall until $\Delta\phi_s$ becomes negligible (which implies that $i_C$ becomes negligible in comparison with $i_H$).

   This changing value of the voltage may be considered to form the zero for the additional voltage due to hydrogen evolution so that the complete equation when the operating current exceeds the instantaneous limiting current is:

$$V = V_{\min} + a_a + b_a \ln i + (iS_e/\gamma_0) + |\Delta\phi_s| + |\eta_{\mathrm{conc, L}}| + |a_H + b_H \ln i_H| \tag{23}$$

It has been assumed that hydrogen evolution is confined to the end of the cathode and that the effect of any gas evolved at either electrode on the behaviour of the reactor system is negligible. In practice gas effects may be dominant but it is still difficult to make a quantitative estimate of the effect of such gas evolution on the behaviour of three-dimensional electrodes.

### 3.3. *Operation below instantaneous limiting current*

In order to determine the cathodic contribution to the overall potential drop for sub-limiting current operation without recourse to complex mathematical forms, the situation has been approximated by a coefficient $\lambda$ which may be defined on one of two ways: either as the constant operating current divided by the instantaneous limiting current

$$\lambda = I/I_L(t) \tag{24}$$

or, in terms of local concentration

$$\lambda = (C - C_s)/C \tag{25}$$

It is shown elsewhere [5] that the definition of $\lambda$ has little effect on the overall applied voltage. Using the alternative definition of $\lambda$ as given by Equation 25 it can be shown [5] that

$$\Delta\phi_s = \frac{zFu^2C_0}{ka\lambda\gamma}\left[\left(1 + \frac{ka\lambda L}{u}\right)\exp\left(-\frac{ka\lambda L}{u}\right) - 1\right] \tag{26}$$

The overall current is in this case obtained as

$$I = zFQC_0\left[1 - \exp\left(-\frac{ka\lambda L}{u}\right)\right] \tag{27}$$

For calculations involving the present batch recirculating system it is important to realise that $\lambda$ itself is time variable. When defined by Equation 4 its numerical value is easily found since $I$ is set and $I_L(t)$ calculated from Equation 4. If defined by Equation 25 $\lambda$ must be found by rearranging Equation 27 to give

$$\lambda(t) = -\frac{u}{kaL}\ln\left\{1 - \frac{I}{zFQC(t)}\right\} \tag{28}$$

where $-u/kaL = 1/(\ln\beta)$ by definition and $C_0(t)$ can be calculated from Equation 9. Once $\lambda$ is known, $\Delta\phi_s$ is found from Equation 26 and $\eta_{\mathrm{conc, L}}$ from Equation 21 by replacing $C_s/C$ with $1 - \lambda$. The

Table 1. *Cell pressure drop components in* $N\,m^{-2}$ *calculated between points* a *and* b *in Fig.1.*

| Re | $H\rho g$ | Bed $\Delta p$ | Entry, exit and bends | Total $\Delta p$ |
|---|---|---|---|---|
| 0.1 | 431.6 | 1.3 | 0.007 | 432.9 |
| 1.0 | 431.6 | 13.22 | 0.21 | 445.1 |
| 10.0 | 431.6 | 154.8 | 2.23 | 588.7 |

remaining terms in Equation 20 are easily determined to give the operating voltage $V(t)$ necessary to maintain the constant operating current for this operating region.

## 4. Energy requirement

The total power at any time is the sum of the electrolysis and cell pumping power consumption.

$$P(t) = V(t)I(t) + \xi Q \Delta p \tag{29}$$

The current is constant in this case except when the system is operated with controlled potential at the instantaneous limiting current for the purposes of comparison.

The energy required per kilogram of copper extracted for 90% conversion in the reservoir is then found using

$$E = P_{av}t_p \tag{30}$$

where the average power consumption, $P_{av}$, is found by numerical integration and the process time, $t_p$ is given by

$$t_p = \frac{t^{90}}{V_R R_f C_0^0 M_w} = \frac{(t^{90}/\tau)}{Q R_f C_0^0 M_w} \tag{31}$$

Values of $\Delta p$ for the cell geometry considered (calculated using the Ergun equation) are given in Table 1. The second term in Equation 29 is negligible in this instance and so power consumption is that for electrolysis only.

## 5. Results and discussion

All results were computed using the packed bed data given in Table 2.

Table 2. *Values of parameters used in computations. Values of* k *were calculated from the equations of Upadhyay and Tripathi [6]*

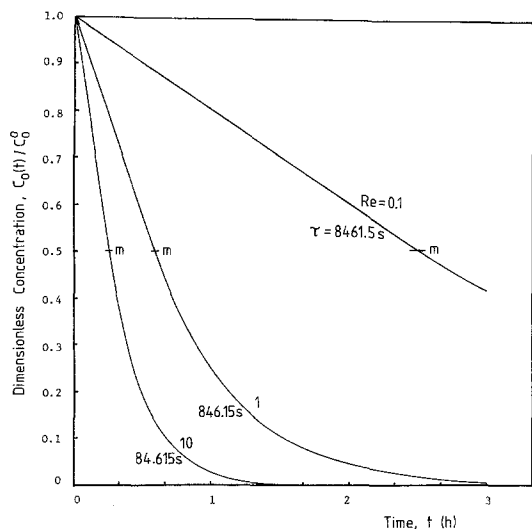| Variable | Value | Variable | Value |
|---|---|---|---|
| $A$ | $10^{-3}\,m^2$ | $Sc$ | 2450 |
| $a$ | $3600\,m^{-1}$ | $V_R$ | $10^{-3}\,m^3$ |
| $L$ | $0.01\,m$ | $V_{min}$ | $0.9\,V$ |
| $z$ | 2 | $R'$ | $8.314\,J\,mol^{-1}\,K^{-1}$ |
| $F$ | $96487\,C\,mol^{-1}$ | $T$ | $298\,K$ |
| $\epsilon$ | 0.4 | $S_e$ | $0.01\,m$ |
| $\gamma_0$ | $50\,ohm^{-1}\,m^{-1}$ | $a_a$ | $0.5\,V$ |
| $C_0^0$ | $10\,mol\,m^{-3}$ | $b_a$ | $0.12\,V$ |
| $\mu$ | $1.3 \times 10^{-3}\,N\,s\,m^{-2}$ | $a_H$ | $-0.24\,V$ |
| $d$ | $10^{-3}\,m$ | $b_H$ | $-0.12\,V$ |
| $\rho$ | $1100\,kg\,m^{-3}$ | | |

Fig. 3. Concentration against time for $\alpha = 0.5$ at various $Re$ (and hence $t/\tau$).

## 5.1. Concentration and current variation

Concentration–time behaviour is illustrated in Fig. 3 for $\alpha = 0.5$ and for three different values of $Re$ (and hence $\tau$). The points marked '$m$' represent the time at which the instantaneous limiting current is exceeded. Naturally an increase in $Re$ leads to a more rapid fall in the reservoir concentration. This fact is obscured by the use of a dimensionless time in the form $t/\tau$ when the curves for $Re = 0.1$ and $Re = 10$ are approximately exchanged. Computations for other values of $\alpha$ are shown elsewhere [5]. The linear fall in concentration initially followed by a more gradual non-linear change is similar in form to the concentration–time curves presented by Wilkinson and Haines [7] for a fluidized bed operated as a recirculating system.

Fig. 4 depicts the instantaneous limiting current–time and operating current–time behaviour for $Re = 1$ and for $\alpha$ values of $0.25, 0.5$ and $0.75$ and also for operation throughout at the instantaneous limiting current. The transition times are again marked as '$m$'. It should be noted that the transition times are not simply the times for the operating current to intersect the limiting current operation curve.
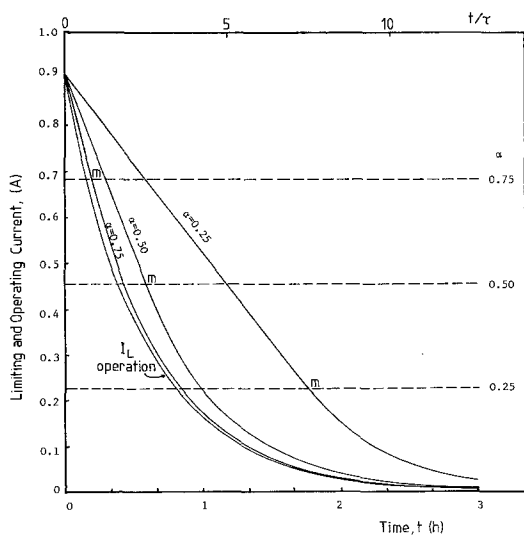


Fig. 4. Limiting (solid lines) and operating (broken lines) currents against time for $Re = 1$ at various $\alpha$ and for limiting operation throughout.
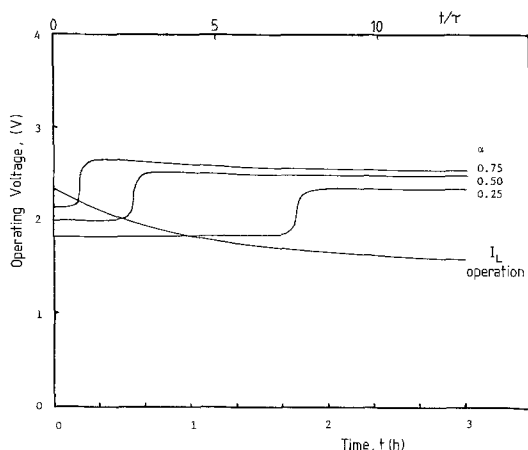
Fig. 5. Operating voltage against time for $Re = 1$ at various $\alpha$ and for limiting operation throughout.

## 5.2. Voltage variation

Shown in Fig. 5 for $Re = 1$ is the voltage–time behaviour of the system for various values of $\alpha$ as well as for limiting current operation. Operation at the instantaneous limiting current throughout results in a fall in voltage as the current falls. Constant current operation under the conditions considered results in an initially approximately constant voltage. Although the solution potential drop within the packed bed falls as the entrance concentration falls, the concentration overpotential rises as the instantaneous limiting current is approached. At high $Re$ however, when the solution potential drop is larger and falls rapidly, a fall in voltage may occur before the instantaneous limiting current is reached since the rise in concentration overpotential is small in comparison. All of the available current is at this stage due to the primary reaction. As the instantaneous limiting current is approached a point is eventually reached at which the mass transfer of $Cu^{2+}$ to the cathode surface is not sufficient to allow the constant operating current to flow and under these conditions Chang et al. [8] have described how the potential of the working electrode must increase to a point at which the current flow can be maintained and the secondary reaction commences. In this case hydrogen evolution occurs and the voltage steps seen in the diagrams are as a result of the increase needed to drive this reaction. It is likely that in practice such sharp increases in voltage would not be observed. A more gradual increase of voltage is probable as parts of the cathode reach conditions for hydrogen evolution. Wilkinson and Haines [7] for a fluidized bed show a voltage–time curve which illustrates an increase in voltage only slightly less steep than those presented here. No attempt has been made to predict the initial sharp drop in voltage which they observed.

## 5.3. Power, energy consumption and process times

The overall power has components due to electrical and pumping requirements, the latter depending on pressure drop. The various components of $\Delta p$ are shown in Table 1. The power due to pumping is very small in the present case compared with that needed for the passage of current. Though the pressure drop could be significant for other systems, in this case the effect of ignoring pumping contributions is less than 0.1%, rising at higher $Re$. Power and voltage would increase if allowance were made for losses in cell connections.

The relationship between energy and process time is shown in Fig. 6 for various values of $\alpha$ and $Re$ and for limiting current operation. The energy is seen to increase rapidly as $\alpha \rightarrow 1$. The disadvantage of decreasing $\alpha$ to reduce energy consumption is that the process time increases. As $\alpha$ is decreased from a value of 1 initially there is little increase in process time but eventually a more rapid increase occurs.
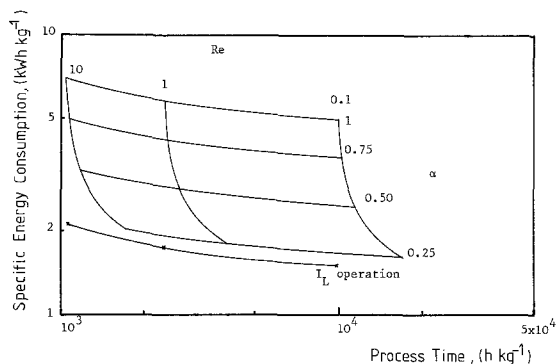
Fig. 6. Specific energy consumption against process time for various $Re$ and $\alpha$ and for limiting operation throughout, assuming 90% conversion in reservoir.

Process times for limiting current operation are of course identical to those for $\alpha = 1$. There is clearly a large increase in process time as $Re$ decreases.

Conflicting objectives therefore exist. To reduce energy consumption requires low $\alpha$ and $Re$. To reduce process time requires high $\alpha$ and $Re$. The relative importance of these two quantities has therefore to be considered for each situation. If for example process time were crucial then it might be possible to make some saving in energy consumption by reducing $\alpha$ provided the process time did not rise significantly. A comparison of predicted energy consumption with available experimental data is shown in Fig. 7 as a function of superficial current density. For the purposes of this comparison higher $Re$ have been used though it should be noted that some of the assumptions are less applicable in this region. In particular for $Re > 50$ the solution potential drop increases dramatically and this may result in highly non-uniform conditions in the cathode. Nevertheless there is general agreement. The data of Wilkinson and Haines [7] were obtained using a side-by-side electrode arrangement and a fluidized bed operated under conditions which suggest a value of $Re$ of about 40. In the case of Scott [9] a moving bed was used while Flett [10] used a fluidized bed of copper-coated glass ballotini (with an electrode arrangement similar to that considered in this work) so that for similar bed expansions $Re$ would be less and the position of the data is in broad agreement with this. The data of Germain and Goodridge [11] are significantly different showing less dependence on superficial current density in the range shown. Their original data show higher values of specific energy consumption at higher and lower values of current density. The poor behaviour of fluidized bed electrodes as the superficial current density falls is given as an explanation of the increase in energy consumption in this region. Thus although the available experimental data are for widely differing systems there is general agreement both among themselves and with the present model. It is worth noting that energy consumption figures of about $2\,kWh\,kg^{-1}$ are reported for copper electrowinning cells with plate electrodes at current densities of $300\,A\,m^{-2}$ [12]. This is also shown on Fig. 7.

## 6. Conclusions

A system with an upstream counter-electrode has been modelled in the present work and results in terms of energy consumption have been shown to be in general agreement with available experimental data. A similar arrangement with a downstream counter-electrode has been shown elsewhere [5] to behave similarly for the copper extraction system considered. Such systems are however known to be impractical for plant use and thus a number of modifications would need to be made to the present model to approximate more closely to side-by-side electrode arrangements such as that used by Wilkinson and Haines [7] in pilot plant studies.

The reactor size chosen in this modelling example is not necessarily realistic and no attempt has been made at a full optimisation of the problem. The emphasis has been to demonstrate a modelling approach to aspects of operating strategy. Fuller analysis would require product value data, equipment (including electrical) capital costs and information concerning interaction with the overall process.
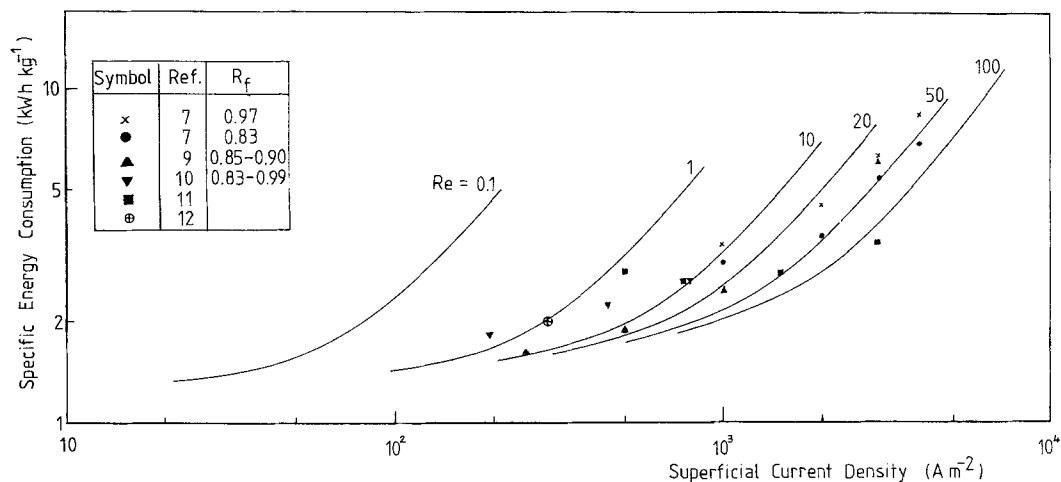
Fig. 7. Specific energy consumption against superficial current density for different $Re$ with $\alpha$ ranging from 0.1 to 1.

## References

[1]  L. H. Mustoe and A. A. Wragg, *J. Chem. Technol. Biotechnol.* **31** (1981) 317.
[2]  A. T. S. Walker and A. A. Wragg, *Electrochim. Acta* **22** (1977) 1129.
[3]  J. Newman and W. Tiedemann, *Adv. Electrochem. Electrochem. Eng.* **11** (1978) 353.
[4]  D. J. Pickett, 'Electrochemical Reactor Design', Elsevier, Amsterdam (1977).
[5]  L. H. Mustoe, Ph.D. Thesis, University of Exeter (1981).
[6]  S. N. Upadhyay and G. Tripathi, *J. Chem. Eng. Data* **20** (1975) 20.
[7]  J. A. E. Wilkinson and K. P. Haines, *Trans. Inst. Min. Metall. C* **81** (1972) 157.
[8]  J. Chang, R. F. Large and G. Popp, 'Techniques of Chemistry,' Vol. 1, Wiley-Interscience, New York (1971) p. 1.
[9]  K. Scott, *J. Appl. Electrochem.* **11** (1981) 339.
[10]  D. S. Flett, *Chem. Ind.* No. 11 (1971) 300.
[11]  S. Germain and F. Goodridge, *Electrochim. Acta* **21** (1976) 545.
[12]  V. A. Ettel and B. V. Tilak, 'Comprehensive Treatise of Electrochemistry', Vol. 2, Plenum Press, New York, (1981) p. 327.